Environ. Sci. Technol. **2002**, *36,* 2154−2163

Evaluation of an Air Quality Model for the Size and Composition of Source-Oriented Particle Classes

PRAKASH V. BHAVE,[†]
MICHAEL J. KLEEMAN,[*,‡]
JONATHAN O. ALLEN,[§] AND
LARA S. HUGHES

Department of Environmental Science and Engineering, California Institute of Technology, Pasadena, California 91125-7800

KIMBERLY A. PRATHER

Department of Chemistry and Biochemistry, University of California, San Diego, La Jolla, California 92093-0314

GLEN R. CASS[#]

School of Earth and Atmospheric Sciences, Georgia Institute of Technology, Atlanta, Georgia 30332-0340

Air quality model predictions of the size and composition of atmospheric particle classes are evaluated by comparison with aerosol time-of-flight mass spectrometry (ATOFMS) measurements of single-particle size and composition at Long Beach and Riverside, CA, during September 1996. The air quality model tracks the physical diameter, chemical composition, and atmospheric concentration of thousands of representative particles from different emissions classes as they are transported from sources to receptors while undergoing atmospheric chemical reactions. In the model, each representative particle interacts with a common gas phase but otherwise evolves separately from all other particles. The model calculations yield an aerosol population, in which particles of a given size may exhibit different chemical compositions. ATOFMS data are adjusted according to the known particle detection efficiencies of the ATOFMS instruments, and model predictions are modified to simulate the chemical sensitivities and compositional detection limits of the ATOFMS instruments. This permits a direct, semiquantitative comparison between the air quality model predictions and the single-particle ATOFMS measurements to be made. The air quality model accurately predicts the fraction of atmospheric particles containing sodium, ammonium, nitrate, carbon, and mineral dust, across all particle sizes measured by ATOFMS at the Long Beach site, and in the coarse particle size range ($D_a \geq 1.8\ \mu$m) at the Riverside site. Given that this model evaluation is very likely the most stringent test of any aerosol air quality model to date, the model predictions show impressive agreement with the single-particle ATOFMS measurements.

* Corresponding author phone: (530)752-8386; fax: (530)752-7872; e-mail: mjkleeman@ucdavis.edu.

[†] Present address: School of Earth & Atmospheric Sciences, Georgia Institute of Technology, Atlanta, GA 30332-0340.

[‡] Present address: Department of Civil & Environmental Engineering, University of California, Davis, CA 95616.

[§] Present address: Departments of Chemical & Materials Engineering and Civil & Environmental Engineering, Arizona State University, Tempe, AZ 82876-6006.

[#] Deceased: July 30, 2001.

Introduction

Particulate matter is distributed by size and composition in the atmosphere. The size and composition distribution of airborne particles determines their deposition efficiency in different regions of the human lung (*1*), their effects on local and regional visibility (*2*), and their large-scale effects on global climate (*3*). Particle size and composition also may indicate the original source of the atmospheric particles (*4*) as well as their toxicity (*5*).

Traditional aerosol processes air quality models do not predict the size and composition of individual atmospheric particles, but rather they predict the *average* chemical composition of particles falling within certain size intervals. Such models include the California Institute of Technology model (CIT) (*6*), the Regional Particulate Matter model (RPM) (*7*), the European Air Pollution Dispersion model (EURAD) (*8*), the Urban Airshed Model-IV with aerosols (UAM-AERO) (*9*, *10*), the Urban Airshed Model-IV with the Aerosol Inorganics Model-2 (UAM-AIM) (*11*, *12*), the Denver Air Quality Model (DAQM) (*13*), the Gas, Aerosol, Transport, and Radiation model (GATOR) (*14*), and the SARMAP Air Quality Model with aerosols (SAQM-AERO) (*15*). Of these, the RPM and EURAD models parametrize the aerosol size distribution as the sum of two or three overlapping log-normal modes, and the remaining models approximate the aerosol size distribution using a sectional representation. All of the models listed above assume that the ambient aerosol is *internally mixed*, meaning all particles in a given size interval or log-normal mode have identical chemical compositions. Several investigators have shown that this internal mixture assumption is inaccurate by observing and reporting significant compositional heterogeneity among ambient particles of the same size (*16*−*18*). Specific cases have been discovered in which modeling the atmospheric aerosol as an internal mixture can misrepresent the evolution of the aerosol size and composition distribution (*19*). Internally mixed aerosol models have the additional disadvantage of masking contributions made by distinct emission sources, because the source identity of the particles is lost when all particles are averaged into a sectional or log-normal aerosol distribution upon emission to the atmosphere. Furthermore, global-scale model calculations (GATOR-GCMM) reveal that the assumptions made regarding the mixing state of ambient aerosols can significantly affect our calculations of the atmospheric radiation budget (*20*).

Recently, we developed an air quality model that overcomes the internal mixture assumption by tracking the evolution of source-oriented particle classes as they undergo atmospheric chemical reactions during transport across a polluted air basin. This model has been used to identify the effect of individual emission sources on ambient air quality (*21*, *22*) and to evaluate the effectiveness of numerous proposed air pollution control strategies on particulate matter concentrations (*23*) and visibility (*24*) in the Southern California region. Model predictions of the overall aerosol size distribution and chemical composition have undergone extensive evaluation and agree favorably with measurements taken during the 1987 Southern California Air Quality Study (*19*, *25*) as well as measurements taken during the 1996 cross-basin trajectory experiment (*26*). Model comparison against

10.1021/es0112700 CCC: $22.00
Published on Web 04/20/2002

TABLE 1: Summary of Source-Oriented Air Quality Model — Lagrangian Formulation

feature	treatment	references
	Spatial and Temporal Dimensions	
spatial scale	urban-scale applications, 5 km × 5 km horizontal grid resolution, five vertical cells	
temporal scale	episodic applications, 1 day − 1 week	
	Aerosol Representation	
chemical species	distinct chemical species in each particle class (EC, OC, NH_4^+, NO_3^-, Na^+, Cl^-, $SO_4^=$, and 30 minor species)	(*28*)
particle size distribution	discrete source-oriented particle classes: 15 initial sizes ranging from 0.01 to 10 μm, from each of 10 emission source categories, emitted during each hour of air parcel transport	
particle size evolution	discrete particles change size as material condenses/evaporates	
particle aging	source-oriented particle classes are segregated by hour of emission	(*25*)
	Emissions	
aerosol phase	size-resolved chemical composition from all major emission sources	(*26, 28*)
gas phase	SO_2, NO, NO_2, NH_3, CO, and over 400 specific organic compounds	(*29*)
	Transport	
advection	horizontal only, based on interpolated wind fields	(*30, 31*)
diffusion	vertical only	(*30*)
vertical wind shear	not included[a]	
	Chemical Mechanisms	
gas-phase chemistry	SAPRC mechanism with extensions: 100 species (O_3, NO_2, NO, N_2O_5, etc.) and 195 reactions	(*32*)
inorganic aerosol thermodynamics	aerosol inorganics module (AIM) with extensions: condensation, evaporation, dissolution, crystallization	(*33, 19*)
organic aerosol thermodynamics	absorption of semivolatile organics into aerosol organic phase	(*34, 35, 23*)
fog kinetic reactions (irreversible)	58 species, 177 reactions	(*36, 37, 19*)
fog equilibrium reactions (reversible)	29 acid−base reactions	(*36, 37, 19*)
	Physical Mechanisms	
dry deposition	surface resistant model with landuse specific parameters	(*30*)
wet deposition	not included[a]	
nucleation	not included[a]	
coagulation	not included[a]	

[a] Process shown to be negligible during current episode (*22*).

ambient single-particle measurements has yet to be attempted. Aerosol time-of-flight mass spectrometry (ATOFMS) data sets that describe ambient single-particle size and composition are available from the 1996 cross-basin trajectory study conducted in Southern California (*27*). The purpose of this paper is to determine how well an air quality model that tracks source-oriented particle classes can account for single-particle characteristics observed in the atmosphere. We present here the first comparison of aerosol processes air quality model predictions with single-particle measurements.

Methods

Description of the Source-Oriented Air Quality Model. The air quality model simulates the most important processes that affect the size and composition distribution of the ambient aerosol. These processes are listed in Table 1. Detailed descriptions of the model structure and formulation can be found elsewhere (*19*, *22*, *25*, *26*). In the model, the ambient aerosol is represented as a source-oriented mixture of particle classes that are released to the atmosphere as primary emissions at 15 discrete particle sizes spanning the 0.01−10 μm particle diameter range. Primary particles are separated into 10 emission source categories: paved road dust, crustal material, diesel engine exhaust, food cooking, catalyst-equipped gasoline-powered engine exhaust, non-catalyst gasoline engine exhaust, sulfur-bearing fuel combustion and industrial sources, sea salt, nonsea salt background particles, and other miscellaneous sources (*19*). The chemical composition of particles emitted from each source category is obtained from the results of emission source sampling experiments. Primary particles emitted from the most important sources in Southern California are represented using chemical composition data that vary by particle size, based on impactor measurements of those emission sources (*38*, *39*). Particles emitted at each discrete size, from each source category, and during each hour along the air parcel trajectory, are tracked separately from all other particle classes in the model. In this manner, a source-oriented mixture of atmospheric particles is created in which all particle classes interact with the same gas-phase conditions, but differences in the size and composition of particles emitted from different sources are retained. Coagulation processes are not included in the present model formulation, because it has been determined that they do not significantly affect the aerosol mass distribution during the episode studied (*22*).

Figure 1a displays an example of the air quality model predictions. The pie chart in Figure 1a quantitatively illustrates the chemical composition of an atmospheric particle class tracked by the air quality model. This particle class contains 15 of the 37 different aerosol phase chemical species that are tracked in the current model formulation. The atmospheric concentration, physical diameter (D_p), and density (ρ) of particles in this class are also calculated in the model, as shown in Figure 1a. Furthermore, each particle class followed by the model is labeled according to the source category from which the particle core was initially emitted and the hour at which the particle was injected into the air parcel. Based on model calculations, the particle class shown in Figure 1a was emitted from a diesel-powered vehicle, 16 h before reaching the receptor site.

In late September and early October, 1996, a field campaign measuring the size distribution and chemical composition of particulate matter was conducted to evaluate the predictions of the air quality model just described (*27*). Instruments were stationed at three sites in the Los Angeles, California area: Long Beach, Fullerton, and Riverside. These monitoring locations were chosen because they lie along a seasonally typical air parcel pathway crossing the Los Angeles Basin. The size and composition distribution of airborne particles and gas-phase pollutant concentrations were measured upwind of the study area at Santa Catalina Island

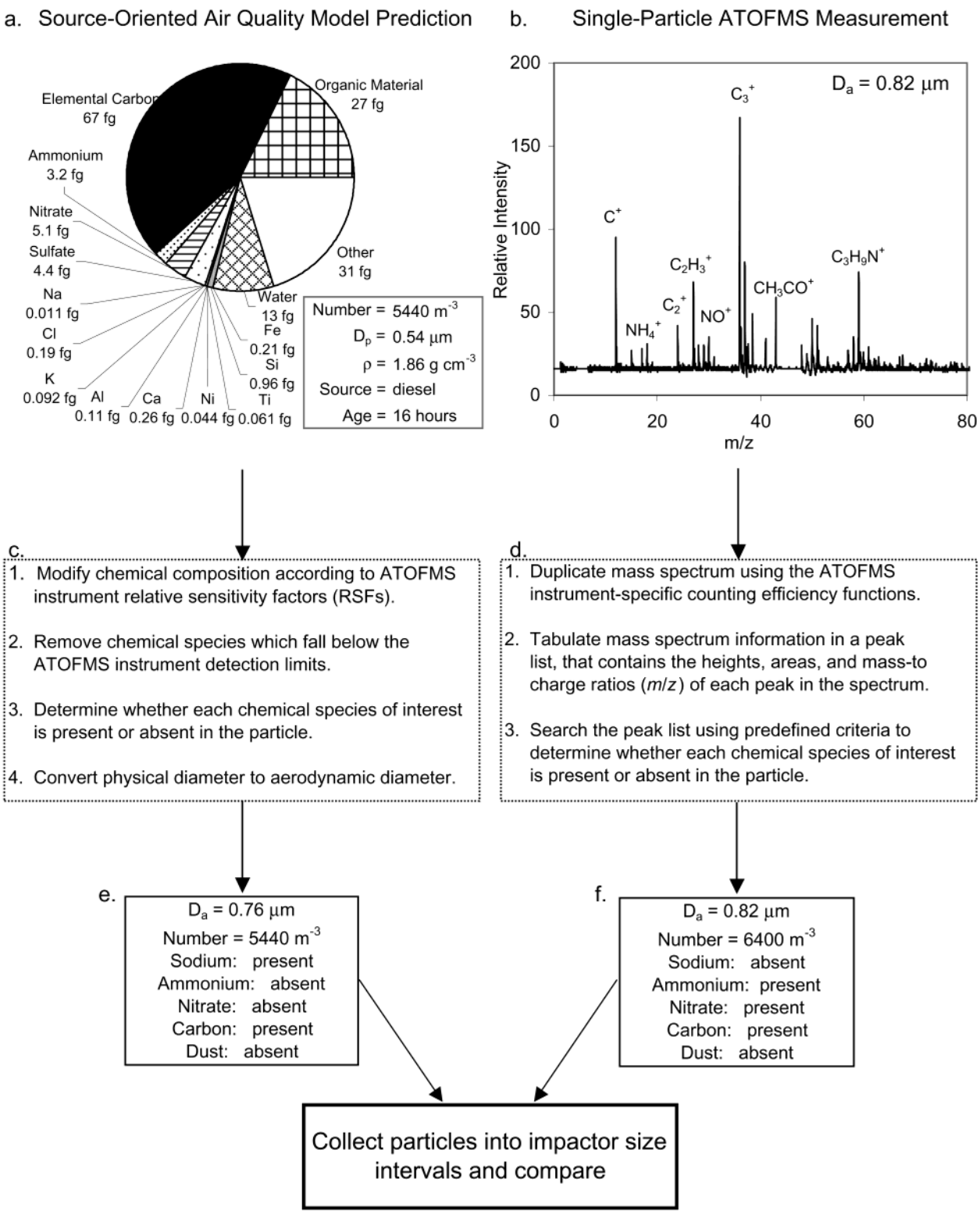

FIGURE 1. Schematic illustration of the model evaluation procedure. (a) Air quality model prediction of a source-oriented particle class arriving at Long Beach on September 24, 1996 (1 fg = 10^{-15}g). (b) Mass spectrum of an ambient particle sampled by ATOFMS at Long Beach, CA on September 24, 1996 (peak intensities are indicated in arbitrary units on the vertical axis). (c−d) Procedures to convert model predictions and single-particle mass spectra into a common format. (e) Resulting particle class description of the model prediction shown in (a). (f) Resulting particle description of the mass spectrum shown in (b).

on September 21−22, 1996, for the purpose of specifying initial conditions to the air quality model. Air parcel trajectories that passed over the Riverside site during the study period were calculated by backward integration through wind fields that were interpolated from wind observations at 29 locations in Southern California (*31*, *40*). Trajectory calculations indicate that the air mass arriving at Riverside during the 1500−1900 PDT intensive sampling period on September 25, 1996, passed over Fullerton between 1430 and 1900 PDT on September 24, 1996, and stagnated near the Long Beach monitoring site during the 0700−1100 PDT intensive sampling period and throughout the morning of

September 24, 1996 (see map in Figure 1b of ref *41*).

The source-oriented air quality model described above was used to predict the size distribution and chemical composition of the airborne particle mixture observed at each of the three air monitoring sites on September 24−25, 1996. Comparison of air quality model predictions to both filter-based and cascade impactor-based measurements of the particle size distribution and bulk chemical composition show good agreement at all three air monitoring sites. We refer the reader to ref *26* for a detailed comparison of the model predictions with filter and impactor measurements taken during the September 24−25, 1996, intensive sampling periods. Briefly, air quality model predictions of fine particulate ($D_a < 1.8\,\mu$m) mass, sulfate, ammonium, and nitrate concentrations as well as total particulate sodium concentrations agree within 35% of filter-based measurements at all three monitoring sites during the episodes studied (see Figure 3 of ref *26*). Furthermore, the air quality model accurately predicts the shapes of the size distributions of fine particulate mass, ammonium, nitrate, and sulfate, at all three monitoring sites (see Figure 4 of ref *26*). Having established confidence in the ability of our air quality model to accurately predict the aerosol size distribution as well as the bulk and size-segregated aerosol chemical composition at all three monitoring sites along the air parcel trajectory, we are prepared to evaluate the air quality model predictions against single-particle measurements.

Description of Single-Particle Aerosol Measurements. On September 24−25, 1996, ATOFMS instruments operated continuously at the Long Beach and Riverside sites. The Long Beach site was equipped with a field-transportable ATOFMS instrument (*42*), and a laboratory-bound ATOFMS instrument (*18*) was stationed at the Riverside site. The ATOFMS instrument located at the Fullerton site was not operated during the September 24−25 time period. Consequently, model predictions of the Fullerton aerosol cannot be evaluated against ATOFMS measurements and will not be discussed in this paper.

A thorough description of the ATOFMS instrument operating principles is provided elsewhere (*18*). Briefly, ambient air is drawn into the ATOFMS instruments, and particles are accelerated to a terminal velocity that is a function of their aerodynamic size. The velocity, hence aerodynamic diameter, of each particle is measured in the sizing chamber by detecting scattered light from two continuous wave timing lasers positioned a fixed distance apart. The arrival time of the sized particle is predicted based on the particle velocity measurement, and a third laser is fired to intercept the sized particle. This third laser ablates and ionizes the contents of the particle and a time-of-flight mass spectrometer analyzes the generated ions, producing a mass spectrum. In this manner, ATOFMS instruments simultaneously measure the chemical composition and size of individual particles. Figure 1b shows the mass spectrum and aerodynamic diameter measurement (D_a) of an individual atmospheric particle sampled using the transportable ATOFMS instrument at Long Beach, during the 1996 trajectory experiment.

At the time of the 1996 trajectory experiment, the ATOFMS instruments could obtain either a positive ion or a negative ion mass spectrum for each particle hit by the ablation/ionization laser. The choice was made to collect positive ion mass spectra throughout the intensive sampling periods described in this paper. As a result, negative ion markers for certain species including sulfate, silicon, and chloride are not available for use in this model evaluation study. Modifications to the transportable ATOFMS instrument design following the 1996 trajectory experiment have added dual ion detection capability, so both positive and negative ion mass spectra are obtained from individual particles in more recent field studies (*43*, *44*).

Model Evaluation Procedure. To evaluate the air quality model predictions, several steps are required to render the ATOFMS measurements and model predictions into a common format that permits a direct comparison to be made. The procedure used to transform ATOFMS measurements into such a format is outlined in Figure 1d. ATOFMS instruments are known to undercount ambient particles by a factor, ϕ, that declines with increasing aerodynamic particle diameter, D_a (*45*)

$$\phi = \alpha D_a^{\beta} \tag{1}$$

where parameters α and β are determined by comparing ATOFMS data with colocated reference measurements. For ATOFMS data collected during the 1996 field experiment, parameter values of α and β are 2133 and −5.527, respectively, for the ATOFMS instrument stationed at Long Beach, and 4999 and −3.236, respectively, for the Riverside-based ATOFMS instrument (*45*). These "counting efficiency" functions were derived for particles smaller than 1.8 μm diameter, because reference measurements at larger particle sizes were not available. To maximize the particle size range over which model predictions can be evaluated in the present study, the ATOFMS counting efficiency functions are extrapolated upward to 3.5 μm. Each particle in the 0.32−3.5 μm aerodynamic diameter range for which a mass spectrum was obtained is "duplicated" in proportion to the degree to which particles of that size were undercounted by the ATOFMS instruments; each particle is assumed to have the same chemical composition as the particle from which it was duplicated. This calculation accounts for the tendency of ATOFMS instruments to preferentially detect large particles rather than smaller ones and results in a particle number distribution matching that of the atmosphere as measured by laser optical particle counters and cascade impactors during the time of sampling (*45*).

Because manual classification of the ATOFMS data is slow, labor intensive, and subject to operator bias (*46*), automated computer software is used to generate a *peak list* that contains the areas, heights, and mass-to-charge (m/z) ratios of all peaks in a particle spectrum. A variety of data analysis programs use these peak lists and the corresponding aerodynamic diameter measurements to group individual particles into meaningful classes. At present, chemical sensitivities of the ATOFMS instruments are not known with sufficient accuracy to quantitatively reconstruct the chemical composition of individual particles. In particular, the magnitude of the instrument response to certain chemical substances may be affected by the presence of other species in the particle matrix. These matrix effects are not well understood at present, so for the current study, particle spectra obtained by ATOFMS are used to indicate only the presence or absence of major chemical species in each particle rather than the quantitative amounts of each chemical component in the particle. The presence or absence of chemical species in each particle can be used to separate the ambient aerosol into compositionally distinct particle classes. Evaluations presented in the current paper compare the presence or absence of selected species in source-oriented model particle classes to the presence or absence of these species in the ATOFMS particle classes.

The presence or absence of sodium, ammonium, nitrate, carbon, and mineral dust, in an individual particle are determined by searching for certain indicator peaks in the peak list corresponding to that particle. The search criteria used to determine whether a particle contains sodium, ammonium, nitrate, and/or carbon, are described by Hughes et al. (*41*). Search criteria for detecting mineral dust in ambient particles were updated for the present paper, based on recent

findings from an ATOFMS single-particle source characterization study of suspended soil samples commonly found in the Southern California region (*47*). The updated mineral dust search criteria are provided in the Supporting Information section of the present paper. All searches of the ATOFMS data are performed using the YAADA data analysis system (www.yaada.org).

By following the procedure outlined in Figure 1d, each mass spectrum acquired by ATOFMS is rendered into the semiquantitative format shown in Figure 1f. The aerodynamic diameter is obtained directly from the ATOFMS measurement, whereas the atmospheric number concentration of particles having the same size and composition as the sampled particle is determined by using the counting efficiency function. The peak list search criteria are used to determine whether the five chemical species of interest were present or absent in the sampled particle. For example, the mass spectrum shown in Figure 1b contains peaks that indicate the presence of ammonium, nitrate, and carbon.

Figure 1c outlines the procedure followed to transform the quantitative air quality model predictions into the semiquantitative ATOFMS data format. The sensitivity of ATOFMS instruments for detecting individual chemical components present in the mixed ambient aerosol varies dramatically from one chemical component to another. For example, recent laboratory work demonstrated that ATOFMS instruments detect K^+ in individual particles with 360 times greater sensitivity than NH_4^+ (*48*). To make an accurate comparison between the air quality model predictions and the single-particle characteristics measured by ATOFMS, the chemical sensitivities and chemical detection limits of the ATOFMS instruments must be accounted for. For the present model evaluation, the air quality model predictions of chemical composition for each source-oriented particle class are modified to simulate the ATOFMS instrument sensitivity to different chemical substances. Mass concentrations of the chemical components within each particle are scaled to reflect the fact that some substances stand out clearly in an ATOFMS single-particle spectrum even when present at very small concentrations within the particle. ATOFMS relative sensitivity factors (RSFs) are defined as the sensitivity of ATOFMS instruments to a species of interest divided by the ATOFMS sensitivity to sodium (*48*). Estimated and experimentally determined RSFs for all chemical species tracked by the air quality model appear in Table 1 of ref *28*. Converting the mass concentrations predicted by the air quality model to molar concentrations and multiplying by the positive ion mode RSFs results in a collection of particles with increased apparent concentrations of chemical species whose RSFs are greater than unity and decreased apparent concentrations of species whose RSFs are less than unity.

After applying the RSFs, the air quality model predictions are further modified to simulate the chemical detection limits of the ATOFMS instruments. In ATOFMS data, species present at very low levels in a particle may not be detectable due to interference from noise in the mass spectrum. In previous ATOFMS studies, a 2% relative peak area threshold has been applied to distinguish real mass spectral peaks from mass spectrometer noise (*49*), where relative peak area is defined as the ratio of the area of a given peak to the total area under the mass spectrum. In an analogous manner, mass spectrometer noise is approximated by discarding model predictions of chemical species whose RSF-adjusted apparent concentrations in an individual particle are less than 2% of the total apparent concentrations of all species in the particle. The 2% chemical detection limit is applied to model predictions in order to determine whether each particle class contains ammonium, nitrate, and/or carbon, in quantities large enough to be detected by the ATOFMS instruments. No detection threshold is applied to categorize particles in the model as sodium-containing because the ATOFMS instruments are thought to be capable of detecting particulate sodium at a level far below the limits of detection of the instruments used to dictate sodium emission inputs to the model. In the model predictions dust-containing particles are identified as such if they originated from the suspension of either crustal material or paved road dust, taking advantage of the air quality model's ability to track the original source of each particle class. In this manner, each particle class tracked by the air quality model is categorized according to whether the class contains sodium, ammonium, nitrate, carbon, and/or mineral dust.

As illustrated on the left-hand side of Figure 1, the detailed, quantitative particle description provided by the air quality model is reduced to an abbreviated, particle description shown in Figure 1e, for the purposes of comparison with the semiquantitative ATOFMS data. The physical particle diameter tracked by the air quality model is converted to aerodynamic diameter using the particle density calculated in the model and assuming that all particles are spherical, whereas the particle number concentration is obtained directly from model predictions. The presence or absence of the five chemical species of interest in each particle is determined after scaling the chemical composition according to ATOFMS instrument RSFs and removing species that fall below the simulated ATOFMS detection limits. In the example shown in Figure 1a, model predictions reveal that the particle contains small amounts of ammonium and nitrate. While simulating the ATOFMS instrument chemical sensitivities and detection limits however, the particle is stripped of its ammonium and nitrate, resulting in the particle description shown in Figure 1e.

After the ATOFMS measurements and air quality model predictions are transformed into a common format, the particles are separated into aerodynamic diameter intervals corresponding to those of the cascade impactors ($D_a = 0.32-0.56\ \mu$m, $0.56-1.0\ \mu$m, $1.0-1.8\ \mu$m, and $1.8-3.5\ \mu$m). Size-segregated and chemically categorized air quality model predictions and ATOFMS measurements can then be directly compared with one another.

Results and Discussion

The remainder of this paper focuses on two 4-h air pollution episodes: (1) 0700−1100 PDT on September 24, 1996, at Long Beach and (2) 1500−1900 PDT on September 25, 1996, at Riverside. As discussed earlier, model predictions of the aerosol size distribution and chemical composition agree favorably with the filter and impactor-based measurements taken at both sites during the indicated time periods (*26*). Moreover, air parcel trajectory calculations revealed that a single air mass passed over both Long Beach and Riverside monitoring sites in succession during the 4-h time periods listed above, as described earlier. Choosing these two sampling periods for the present study enables us to evaluate air quality model predictions of the evolution of a source-oriented particle mixture within a single air parcel as it is transported across the Los Angeles area. For these reasons, we have chosen to focus the current model evaluation study on the two indicated time periods.

In this section, air quality model predictions and ATOFMS measurements are compared for the two time periods of interest. ATOFMS instruments obtained positive ion mass spectra from 4780 particles with $D_a = 0.56-3.5\ \mu$m during the 4-h intensive sampling period at Long Beach and 3517 particles with $D_a = 0.32-3.5\ \mu$m during the intensive sampling period at Riverside. Model predictions are obtained by computing pollutant evolution along trajectories terminating hourly at each monitoring site and then pooling the model results from each trajectory over the 4-h intensive sampling periods. The air quality model tracked the evolution of 2388

source-oriented particle classes reaching the Long Beach site with $D_a = 0.56-3.5\ \mu$m during the time period of interest and 8872 particle classes with $D_a = 0.32-3.5\ \mu$m reaching the Riverside site. Model predictions will be compared with ATOFMS measurements of size-segregated chemical composition in two steps. First, we will compare the fraction of particles in each size interval that contain one or more of the five chemical species of interest. These will be referred to as *single-component* comparisons because the model predictions will be compared with ATOFMS measurements one chemical component at a time. Next we will compare the compositional heterogeneity of the size-segregated particle populations predicted by the air quality model and measured by the ATOFMS instruments at both sites. These will be referred to as *multicomponent* comparisons because model predictions of the fraction of particles consisting of unique combinations of chemical species will be compared with ATOFMS measurements.

Single-Component Model Evaluation. Figure 2 displays the fraction of particles in each size interval containing any one of the five chemical species of interest. Air quality model predictions are plotted as black stars, and ATOFMS measurements are plotted as solid lines. The left column of Figure 2 depicts the single-component comparisons at the Long Beach monitoring site. Trajectory calculations indicate that the air parcels studied here spent between 13 and 17 h over land before reaching the Long Beach site during the time period of interest. The aerosol sampled at Long Beach had therefore undergone significant atmospheric processing in the polluted region upwind of Long Beach, and the degree of atmospheric processing is simulated accurately by the air quality model. The model accurately predicts an abundance of sodium-containing and nitrate-containing particles with $D_a = 1.8-3.5\ \mu$m and an abundance of ammonium-containing, nitrate-containing, and carbon-containing particles in the $1.0-1.8\ \mu$m and $0.56-1.0\ \mu$m size ranges. The air quality model accurately calculates that mineral dust is present in a relatively small fraction of the ambient particles in all three size ranges studied. Overall, air quality model predictions and ATOFMS measurements at the Long Beach site are in excellent agreement with one another for all five chemical species of interest across the entire particle size range measured by the transportable ATOFMS instrument.

The right-hand column of Figure 2 depicts single-component comparisons between the air quality model predictions and ATOFMS measurements at the Riverside monitoring site. Overall, model predictions are in good agreement with ATOFMS measurements in the largest particle size range measured at Riverside, but there is less agreement at smaller particle diameters.

In the $1.8-3.5\ \mu$m size range, the air quality model accurately predicts the percentage of particles that contain sodium, nitrate, carbon, and mineral dust, as shown in the upper right-hand subplot of Figure 2. The ammonium-containing particle fraction predicted by the air quality model in the $1.8-3.5\ \mu$m size range is almost three times as large as that measured by the ATOFMS instrument at Riverside. The high ammonium-containing particle fraction predicted by the air quality model is caused primarily by a large ammonia source located in the Chino dairy area upwind of the Riverside site as well as many smaller ammonia sources located throughout the Los Angeles region. The filter and impactor measurements of particulate ammonium mass concentration at Riverside during the sampling period reinforce the predictions of the air quality model (*26*). One possible explanation for the difference between the model predictions and ATOFMS measurements is that the ATOFMS instrument may be less sensitive to detecting ammonium ions in atmospheric particles than was previously assumed.

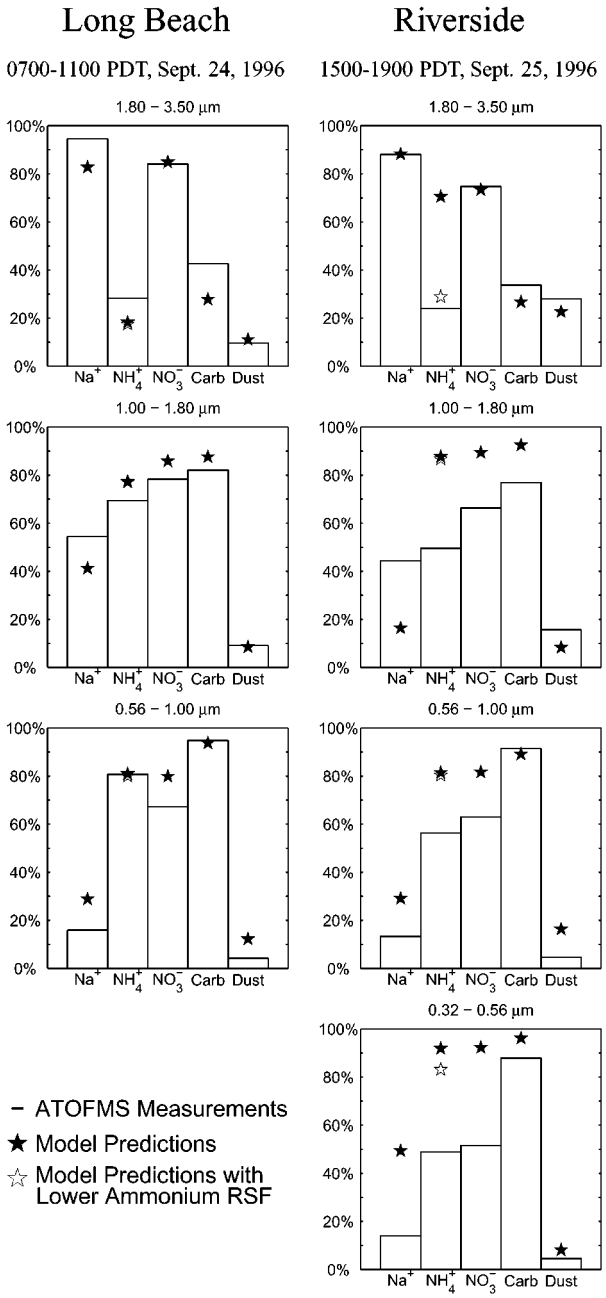

FIGURE 2. Single-component comparisons of model predictions and ATOFMS measurements. Vertical axes indicate the fraction of particles in the given particle size interval that contain the chemical component of interest. The transportable ATOFMS instrument stationed at Long Beach did not sample a sufficient number of particles smaller than 0.56 μm to warrant a comparison in the 0.32–0.56 μm size range.

The ammonium ion RSF applied to model predictions in the current study is based on laboratory measurements of aerosol generated from equimolar solutions of NaCl and NH_4Cl (*48*). Ammonium in the $1.8-3.5\ \mu$m range at Riverside is present primarily in the form of NH_4NO_3, not NH_4Cl, raising the possibility that the ammonium ion RSF may be inapplicable to the ambient aerosol studied here. We can simulate a reduced sensitivity to ammonium by lowering the ammonium ion RSF applied to the model predictions by a factor of 2. Model predictions of the ammonium-containing particle fraction, modified by this lower ammonium ion RSF, are displayed as white stars in Figure 2. This RSF reduction brings model predictions into agreement with ATOFMS measurements of the ammonium-containing particle fraction in the

1.8−3.5 μm size range at Riverside and slightly improves agreement in the 0.32−0.56 μm size range. Furthermore, the reduced ammonium ion RSF does not significantly affect model performance at the Long Beach site across all of the size ranges studied. This lends credence to the hypothesis that ATOFMS sensitivity to ammonium is lower in the ambient aerosol studied here than in the laboratory-generated aerosol from which the ammonium ion RSF was determined. The sensitivities of ATOFMS instruments to various chemical species under ambient sampling conditions are currently being determined to allow more refined comparisons of ATOFMS measurements with air quality model predictions in the future.

In the smallest three size ranges studied at the Riverside site, model predictions show less agreement with the single-particle ATOFMS measurements. The most noticeable difference is that the model predicts much larger ammonium-containing and nitrate-containing particle fractions to be present in the fine particle size intervals (D_a < 1.8 μm) than what the ATOFMS measured. Some of this difference can be mitigated by reducing the ammonium ion RSF as discussed above. However, this still leaves air quality model predictions of both ammonium and nitrate in excess of the ATOFMS measurements in the fine particle size range. Analysis of the single-particle ATOFMS measurements at the Riverside site reveal a large class of fine carbonaceous particles that contains neither ammonium nor nitrate. This particle class appears to be from fresh combustion source emissions which did not have time to accumulate ammonium nitrate before being sampled by the ATOFMS instrument. The laboratory-based ATOFMS instrument was stationed on the second floor of Pierce Hall at the University of California, Riverside, which unfortunately was located near the loading docks for the campus cafeteria and bookstore. At the time of sampling, the bookstore was receiving more deliveries than usual due to the start of the fall academic term. In addition, a strong food cooking smell was noted at the sampling site during the study period, possibly due to cafeteria operations upwind of the sampling equipment. The number of purely carbonaceous particles measured by ATOFMS dropped off by a factor of 2 after 1700 PDT on September 25, possibly corresponding with the end of the business day for the campus cafeteria and bookstore. The largest difference between the model predictions and ATOFMS measurements of the ammonium-containing and nitrate-containing particle fractions at Riverside is noted in the smallest measured size range (D_a = 0.32−0.56 μm), which corresponds with the peak in the aerosol size distributions of freshly emitted motor vehicle exhaust and emissions from meat cooking operations (*38*, *39*). For all of the reasons listed above, vehicle exhaust from the loading docks and food cooking particles from the cafeteria are both likely sources of the purely carbonaceous aerosol measured by ATOFMS at Riverside. The air quality model operates using a horizontal spatial resolution of 5 km × 5 km and is therefore unable to resolve emissions from sources located very near a monitoring site. However, large quantities of gas-phase ammonia and nitric acid measured at the Riverside site during the sampling period (*41*) support the air quality model predictions that most of the aged particles in the fine particle size range must have accumulated ammonium nitrate before reaching the Riverside monitoring site.

The fractions of particles predicted to contain dust by the air quality model in the 0.32−1.0 μm size range at Riverside and in the 0.56−1.0 μm size range at Long Beach are larger than the corresponding dust-containing particle fractions measured by ATOFMS. Sodium-containing particle fractions predicted by the air quality model in these size ranges are also larger than the corresponding ATOFMS measurements. Chemical composition profiles of both crustal material and paved road dust contain sodium (*50*), suggesting that these two differences may be associated with one another. Due to the unavailability of size-distributed measurements of suspended crustal material and paved road dust, the submicron size distributions of these two aerosol emission sources used in the air quality model are obtained from ambient impactor measurements of the nonhygroscopic particle fraction taken at Claremont, CA (*17*). To improve the ability of our air quality model to predict the soil-containing and sodium-containing particle fractions in the submicron size range, a detailed characterization of the size and composition distribution of both crustal material and paved road dust is warranted. The presence of near-field sources of fresh carbonaceous particles at the Riverside site, discussed above, reduce the dust-containing and sodium-containing particle fractions measured by ATOFMS, further contributing to the disagreement between the ATOFMS measurements and air quality model predictions in the fine particle size range (D_a < 1.8 μm).

Multicomponent Model Evaluation. After noting the general agreement between model predictions and ATOFMS measurements in the single-component comparison, the air quality model predictions are subjected to an even more stringent evaluation. All particles in the air quality model predictions and in the ATOFMS data set which contain the same combination of chemical species are grouped together and compared against one another. Figure 3 shows the results of this multicomponent comparison as a color-coded display, illustrating the chemical heterogeneity among size-segregated particles as predicted by the air quality model and as measured by the ATOFMS instruments at the Long Beach and Riverside sites. Each of the 100 dots within a square plot in Figure 3 represents 1% of the particle population at the time and location indicated, within the specified aerodynamic particle diameter range. Each dot is striped with colors that correspond to the chemical components found in 1% of the size-segregated particle population. The exception to this rule is the dust particle category; all mineral dust-containing particles are represented as solid gray dots because the ATOFMS ion peaks associated with dust often have areas so large that they exceed the instrument's dynamic range and produce noise in the rest of the mass spectrum, making the detection of other peaks less reliable. Therefore, any or all of the other chemical species may be present within the mineral dust-containing particles represented by a solid gray dot. As a result, the gray dots in Figure 3 relay the same information depicted by the corresponding stars and solid lines in Figure 2. In Figure 3, a color stripe only qualitatively indicates the presence of the corresponding chemical species; no conclusions should be drawn about the relative amounts of each chemical substance in a particle. The "many types" category, shown in green, is the sum of those particle types which each encompass less than approximately 0.5% of the particle population and which would therefore not warrant representation by an entire dot. The comparisons displayed in Figure 3 are tabulated numerically in the Supporting Information.

The ATOFMS measurements displayed in Figure 3 are identical to those that appear in Figure 8h−n of ref *41*, with the exception that the mineral dust search criteria updated for the present study results in a larger fraction of particles being classified as "dust" across all size ranges and at both monitoring sites. The model predictions shown in Figure 3 are obtained by following the procedures described above, and the RSF applied to model predictions of ammonium ions at both sites and all particle size ranges is reduced by a factor of 2. This adjustment was made to simulate a lower ATOFMS instrument sensitivity to ammonium ions in ambient particles, as inferred from analysis of the single-component comparisons presented earlier.

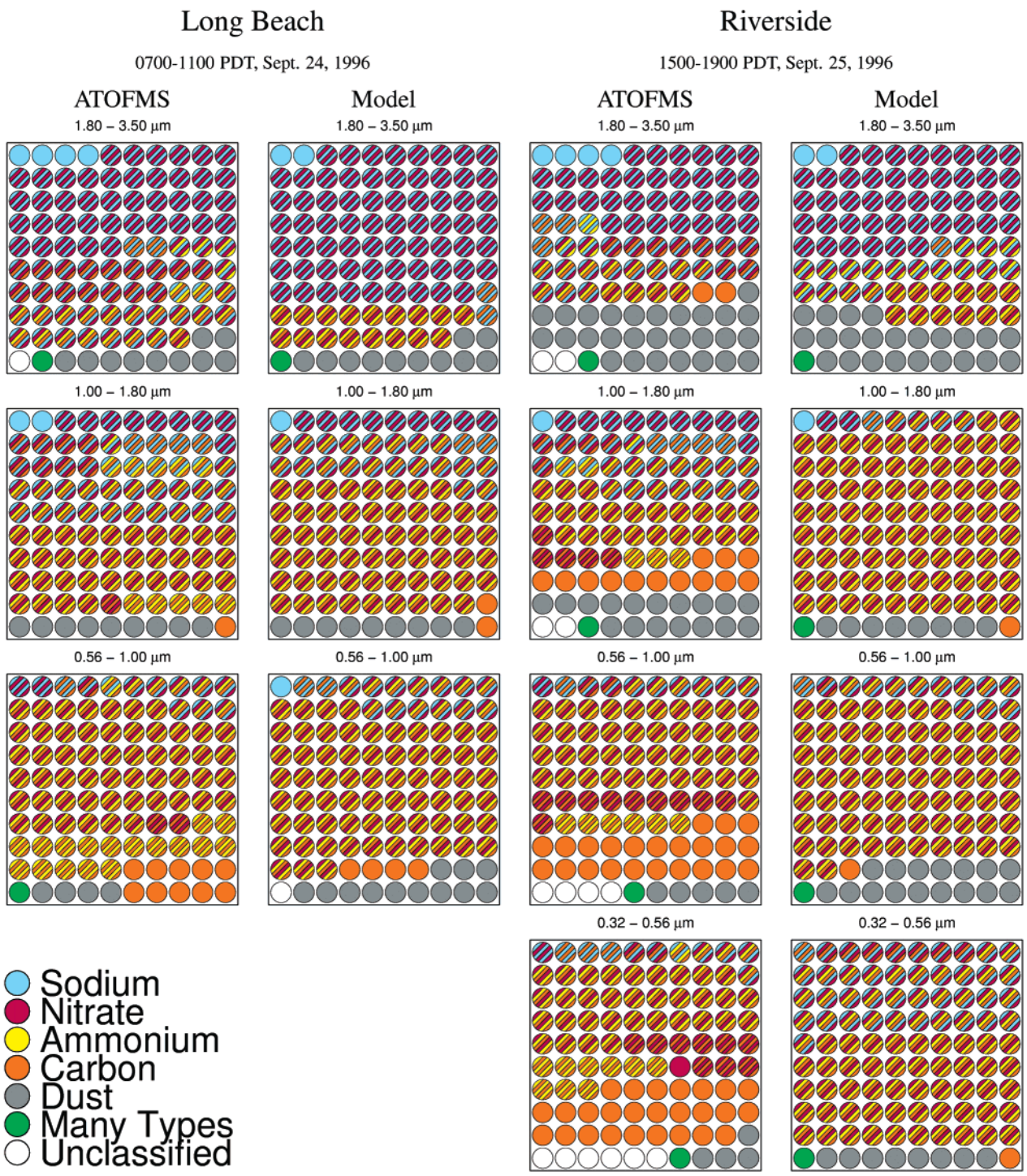

FIGURE 3. Multicomponent comparisons of model predictions and ATOFMS measurements. Each dot represents 1% of the particle population within the indicated aerodynamic particle diameter range. The transportable ATOFMS instrument stationed at Long Beach did not sample a sufficient number of particles smaller than 0.56 μm to warrant a comparison in the 0.32−0.56 μm size range.

The left half of Figure 3 displays multicomponent comparisons between air quality model predictions and ATOFMS measurements at the Long Beach site. In the 1.8−3.5 μm size range, the model accurately predicts the presence of sodium and nitrate (represented by blue and red stripes) on the vast majority of particles. Model calculations indicate that these particles originated as sea spray. Likewise, ATOFMS spectra associated with the sodium and nitrate-containing particle class in the 1.8−3.5 μm size range contain indicator peaks that commonly result from sea spray particles. This suggests that the model accurately calculates the relative contribution of sea spray aerosols to the particle number concentration in this size range. The air quality model also accurately predicts a small fraction of particles containing sodium and carbon which have not accumulated ammonium nitrate. These particles are represented by blue and orange striped dots. Model calculations suggest that these particles were emitted from motor vehicles near the Long Beach site during the morning rush hour traffic period. Model predictions of the dust-containing particle fraction (solid gray dots) are in excellent agreement with the ATOFMS measurements in the 1.8−3.5 μm size range. This agreement lends credence to the emission inventories of paved road dust and crustal material, used as input to the air quality model.

ATOFMS measurements reveal that 16% of the particles in the 1.8−3.5 μm size range at Long Beach contain carbon, sodium, and nitrate (orange, blue, and red striped dots), whereas air quality model predictions for the same size range at Long Beach do not contain this particle type. Analyses of the associated single-particle measurements indicate that this class of particles originated as sea spray. In the air quality model calculations, sea spray aerosols are initialized as an internal mixture of sodium, chloride, and nitrate (*26*), and these particles do not accumulate sufficient amounts of secondary organic material during transport between the coastline and Long Beach to exceed the simulated ATOFMS detection threshold for carbon. This suggests that the carbon detected by ATOFMS in these particles may be primary in nature. Although it is not possible to discern from the Long Beach ATOFMS data whether this sea salt-associated carbon is primary or secondary, recent single-particle measurements of clean marine air indicate that a large fraction of sea salt particles contain primary organic carbon (*51*). In the future, it may be possible to seed the air quality model with multiple classes of sea spray aerosol, each having a distinct chemical composition. This will very likely improve the agreement between model predictions and ATOFMS measurements of the coarse mode carbon-containing particle fraction. The air quality model predictions show 17% of the particles in the 1.8−3.5 μm size range contain ammonium, nitrate, and carbon (red, orange, and yellow striped dots), but they lack sodium. This particle type composes only 1% of the ATOFMS data. Instead the ATOFMS data shows 18% of particles in the coarse size range containing sodium, nitrate, ammonium, and carbon (blue, red, yellow, and orange striped dots). The likely cause of this difference is that ATOFMS instruments are extremely sensitive to the sodium ion and therefore detect sodium in particles from emission sources for which the model's emission source profiles contain no sodium.

In the 1.0−1.8 μm size range at Long Beach, the model continues to meet the stringent multicomponent evaluation. Model predictions of particles containing sodium only (solid blue dots), sodium and nitrate (blue and red striped dots), sodium and nitrate and ammonium and carbon (blue, red, yellow, and orange striped dots), carbon only (solid orange dots), and mineral dust (solid gray dots), all match the measurements of the ATOFMS instrument within 1%. The close agreement between model predictions and ATOFMS measurements of the particle class containing sodium, nitrate, ammonium, and carbon suggests that the ammonium nitrate formation and partitioning processes within the model are relatively accurate. The only noteworthy difference between model predictions and ATOFMS measurements in the 1.0−1.8 μm size range at Long Beach is the excess quantity of particles containing ammonium, nitrate, and carbon in the model predictions (red, orange, and yellow striped dots). This difference is to be expected based on the single-component comparison, which showed that the model somewhat overpredicts the ammonium-containing, nitrate-containing, and carbon-containing particle fractions in the 1.0−1.8 μm size range (see Figure 2).

The air quality model accurately predicts that the most common particle type present in the 0.56−1.0 μm size range at Long Beach contains ammonium, nitrate, and carbon (red, orange, and yellow striped dots). The air quality model also predicts the presence of three compositionally distinct sodium-containing particle types, agreeing fairly well with the chemical heterogeneity of sodium-containing particles measured by ATOFMS. The overprediction of dust-containing particles (solid gray dots) by the air quality model in the 0.56−1.0 μm size range at Long Beach was discussed in conjunction with the single-component comparison. The only other apparent difference between the model predictions and ATOFMS measurements at Long Beach in the 0.56−1.0 μm size range is the lack of a particle type containing only carbon and ammonium (orange and yellow striped dots) in the model predictions. Instead, the model predicts an excess of particles containing ammonium, nitrate, and carbon (red, orange, and yellow striped dots). The absence of nitrate in the ATOFMS measurements of the particle type containing only carbon and ammonium may be due to the fact that only positive ion mass spectra were collected during the 1996 field experiment. ATOFMS instruments are known to be more sensitive to nitrate when operating in the negative ion mode than when operating in the positive ion mode. The availability of dual polarity ATOFMS data in more recent field experiments may yield better agreement between model predictions and ATOFMS measurements of the nitrate-containing particle fraction.

The right half of Figure 3 documents the multicomponent comparisons between model predictions and ATOFMS measurements at the Riverside site. In the 1.8−3.5 μm size range, the air quality model accurately predicts that the most common particle types at Riverside contain either sodium and nitrate (blue and red striped dots) or mineral dust (solid gray dots). The air quality model predicts that seven compositionally distinct particle types are present in quantities greater than 0.5% of the particle population in the 1.8−3.5 μm size range at Riverside. ATOFMS measurements in the same particle size range display 10 compositionally distinct particle types at the Riverside site. Comparing the number of distinct particle types serves as yet another measure of the model's ability to represent the complex mixtures present in the polluted ambient aerosol. The multicomponent comparisons in the fine particle size range (D_a < 1.8 μm) studied at Riverside are very likely affected by the presence of combustion sources located near the ATOFMS instrument during the sampling period, and therefore will not be discussed in detail.

Evolution of the Aerosol Mixture. Taken as a whole, Figure 3 displays the ability of the air quality model to represent the urban aerosol as a population of source-oriented particle classes and to calculate how that particle population changes due to emissions of new particles, dry deposition, and atmospheric reactions, as it is transported across the Los Angeles urban area. Most coarse particles (D_a > 1.8 μm) in the air parcel studied here contain sodium and nitrate at Long Beach. As the air parcel traverses the Los Angeles urban area, it picks up significant quantities of mineral dust material. The particles which originally contained sodium and nitrate (blue and red striped dots) accumulate ammonium, nitrate, and carbon, due to gas-to-particle conversion processes. At first glance, the smaller particles studied here (D_a < 1.8 μm) appear to undergo a less pronounced evolution than their coarse mode counterparts, based on the color-coded display shown in Figure 3. However, Figure 3 does not display the relative *amounts* of the various chemical species present on the atmospheric particles. The air quality model predicts substantial increases in the amounts of ammonium, nitrate, and organic carbon on fine particles over time. As the quantification ability of single-particle instruments is improved, it may be possible in the future to quantitatively evaluate model predictions of the relative amounts of various chemical substances present in source-oriented particle classes.

While the results of the multicomponent comparisons presented in this study are promising, it appears that the air quality model somewhat underpredicts the number of compositionally distinct particle types present in the urban aerosol, as compared to the number of distinct particle types measured by the ATOFMS instruments. One possible explanation for this underprediction is that some of the particle types measured by ATOFMS may have resulted from the coagulation of two or more particles that were emitted from

different source types. Coagulation processes are not included in the current model formulation, but they may be necessary to improve the accuracy of model predictions in future applications. Another possible explanation for the under-prediction of ambient particle heterogeneity is that the emissions inputs to the air quality model are represented as source-specific internal mixtures, where all particles emitted from a certain source type at a given size are assumed to have identical chemical compositions. Recent ATOFMS studies reveal that primary particles of the same size emitted from a single emission source actually exhibit different chemical compositions (*47*, *52*, *53*). In future work, the emissions inputs to the air quality model may be represented as mixtures of compositionally distinct particle types by incorporating the results of detailed single-particle emission source characterization studies that are currently underway.

Acknowledgments

This research was supported by the U.S. Environmental Protection Agency under agreement No. R826371-01-0. Thanks are due to Don-Yuan Liu and Keith Coffee from the University of California at Riverside and Philip Silva from Aerodyne Research, Inc., for their assistance with this work.

Supporting Information Available

Search criteria for detecting mineral dust in ATOFMS ambient particle spectra and a numerical tabulation of the multi-component model evaluation displayed in Figure 3. This material is available free of charge via the Internet at http://pubs.acs.org.

Literature Cited

(1) Yu, C. P. *Powder Technology* **1978**, *21*, 55−62.
(2) National Research Council. *Protecting Visibility in National Parks and Wilderness Areas*; National Academy Press: Washington, DC, 1993.
(3) Charlson, R. J.; Schwartz, S. E.; Hales, J. M.; Cess, R. D.; Coakley, J. A.; Hansen, J. E.; Hofmann, D. J. *Science* **1992**, *255*, 423−430.
(4) Hopke, P. K. In *Receptor Modeling for Air Quality Management*; Hopke, P. K., Ed.; Elsevier Science Publishers: Amsterdam, 1991; pp 1−10.
(5) Harrison, R. M.; Yin, J. *Sci. Total Environ.* **2000**, *249*, 85−101.
(6) Meng, Z.; Dabdub, D.; Seinfeld, J. H. *J. Geophys. Res.* **1998**, *103*, 3419−3435.
(7) Binkowski, F. S.; Shankar, U. *J. Geophys. Res.* **1995**, *100*, 26191−26209.
(8) Ackermann, I. J.; Hass, H.; Memmesheimer, M.; Ebel, A.; Binkowski, F. S.; Shankar, U. *Atmos. Environ.* **1998**, *32*, 2981−2999.
(9) Wexler, A. S.; Lurmann, F. W.; Seinfeld, J. H. *Atmos. Environ.* **1994**, *28*, 531−546.
(10) Lurmann, F. W.; Wexler, A. S.; Pandis, S. N.; Musarra, S.; Kumar, N.; Seinfeld, J. H. *Atmos. Environ.* **1997**, *31*, 2695−2715.
(11) Potukuchi, S.; Wexler, A. S. *Atmos. Environ.* **1997**, *31*, 741−753.
(12) Sun, Q.; Wexler, A. S. *Atmos. Environ.* **1998**, *32*, 3533−3545.
(13) Middleton, P. *J. Air Waste Management Assoc.* **1997**, *47*, 302−316.
(14) Jacobson, M. Z. *Atmos. Environ.* **1997**, *31*, 131−144.
(15) Pai, P.; Vijayaraghavan, K.; Seigneur, C. *J. Air Waste Management Assoc.* **2000**, *50*, 32−42.
(16) McMurry, P. H.; Stolzenburg, M. R. *Atmos. Environ.* **1989**, *23*, 497−507.
(17) Zhang, X. Q.; McMurry, P. H.; Hering, S. V.; Casuccio, G. S. *Atmos. Environ.* **1993**, *27A*, 1593−1607.
(18) Noble, C. A.; Prather, K. A. *Environ. Sci. Technol.* **1996**, *30*, 2667−2680.
(19) Kleeman, M. J.; Cass, G. R.; Eldering, A. *J. Geophys. Res.* **1997**, *102*, 21355−21372.
(20) Jacobson, M. Z. *Science* **2001**, *409*, 695−697.
(21) Kleeman, M. J.; Cass, G. R. *Atmos. Environ.* **1999**, *33*, 4597−4613.
(22) Kleeman, M. J.; Cass, G. R. *Environ. Sci. Technol.* **2001**, *35*, 4834−4848.
(23) Kleeman, M. J.; Cass, G. R. *Environ. Sci. Technol.* **1999**, *33*, 177−189.
(24) Kleeman, M. J.; Eldering, A.; Hall, J. R.; Cass, G. R. *Environ. Sci. Technol.* **2001**, *35*, 4668−4674.
(25) Kleeman, M. J.; Cass, G. R. *Atmos. Environ.* **1998**, *32*, 2803−2816.
(26) Kleeman, M. J.; Hughes, L. S.; Allen, J. O.; Cass, G. R. *Environ. Sci. Technol.* **1999**, *33*, 4331−4341.
(27) Hughes, L. S.; Allen, J. O.; Kleeman, M. J.; Johnson, R. J.; Cass, G. R.; Gross, D. S.; Gard, E. E.; Gälli, M. E.; Morrical, B. D.; Fergenson, D. P.; Dienes, T.; Noble, C. A.; Liu, D.-Y.; Silva, P. J.; Prather, K. A. *Environ. Sci. Technol.* **1999**, *33*, 3506−3515.
(28) Bhave, P. V.; Fergenson, D. P.; Prather, K. A.; Cass, G. R. *Environ. Sci. Technol.* **2001**, *35*, 2060−2072.
(29) Eldering, A.; Cass, G. R. *J. Geophys. Res.* **1996**, *101*, 19343−19369.
(30) Russell, A. G.; McRae, G. J.; Cass, G. R. *Atmos. Environ.* **1983**, *17*, 949−964
(31) Goodin, W. R.; McRae, G. J.; Seinfeld, J. H. *J. Appl. Meteor.* **1979**, *18*, 761−771.
(32) Pandis, S. N.; Harley, R. A.; Cass, G. R.; Seinfeld, J. H. *Atmos. Environ.* **1992**, *26A*, 2269−2282.
(33) Wexler, A. S.; Seinfeld, J. H. *Atmos. Environ.* **1991**, *25A*, 2731−2748.
(34) Odum, J. R.; Jungkamp, T. P. W.; Griffin, R. J.; Flagan, R. C.; Seinfeld, J. H. *Science* **1997**, *276*, 96−99.
(35) Odum, J. R.; Jungkamp, T. P. W.; Griffin, R. J.; Forstner, H. J. L.; Flagan, R. C.; Seinfeld, J. H. *Environ. Sci. Technol.* **1997**, *31*, 1890−1897.
(36) Jacob, D. J. *J. Geophys. Res.* **1986**, *91*, 9807−9826.
(37) Jacob, D. J.; Gottlieb, E. W.; Prather, M. J. *J. Geophys. Res.* **1989**, *94*, 12975−13002.
(38) Kleeman, M. J.; Schauer, J. J.; Cass, G. R. *Environ. Sci. Technol.* **1999**, *33*, 3516−3523.
(39) Kleeman, M. J.; Schauer, J. J.; Cass, G. R. *Environ. Sci. Technol.* **2000**, *34*, 1132−1142.
(40) Harley, R. A.; Russell, A. G.; McRae, G. J.; Cass, G. R.; Seinfeld, J. H. *Environ. Sci. Technol.* **1993**, *27*, 378−388.
(41) Hughes, L. S.; Allen, J. O.; Bhave, P.; Kleeman, M. J.; Cass, G. R.; Liu, D.-Y.; Fergenson, D. P.; Morrical, B. D.; Prather, K. A. *Environ. Sci. Technol.* **2000**, *34*, 3058−3068.
(42) Gard, E.; Mayer, J. E.; Morrical, B. D.; Dienes, T.; Fergenson, D. P.; Prather, K. A. *Anal. Chem.* **1997**, *69*, 4083−4091.
(43) Guazzotti, S. A.; Whiteaker, J. R.; Suess, D.; Coffee, K. R.; Prather, K. A. *Atmos. Environ.* **2001**, *35*, 3229−3240.
(44) Guazzotti, S. A.; Coffee, K. R.; Prather, K. A. *J. Geophys. Res.* **2001**, *106*, 28607−28627.
(45) Allen, J. O.; Fergenson, D. P.; Gard, E. E.; Hughes, L. S.; Morrical, B. D.; Kleeman, M. J.; Gross, D. S.; Gälli, M. E.; Prather, K. A.; Cass, G. R. *Environ. Sci. Technol.* **2000**, *34*, 211−217.
(46) Fergenson, D. P.; Liu, D.-Y.; Silva, P. J.; Prather, K. A. *Chemom. Intell. Lab.* **1997**, *37*, 197−203.
(47) Silva, P. J.; Carlin, R. A.; Prather, K. A. *Atmos. Environ.* **2000**, *34*, 1811−1820.
(48) Gross, D. S.; Gälli, M. E.; Silva, P. J.; Prather, K. A. *Anal. Chem.* **2000**, *72*, 416−422.
(49) Liu, D.-Y.; Prather, K. A.; Hering, S. V. *Aerosol Sci. Technol.* **2000**, *33*, 71−86.
(50) Houck, J. E.; Chow, J. C.; Watson, J. G.; Simons, C. A.; Pritchett, L. C.; Goulet, J. M.; Frazier, C. A. *Determination of Particle Size Distribution and Chemical Composition of Particulate Matter from Selected Sources in California*; Final report to California Air Resources Board; OMNI Environmental Services, Inc.: Beaverton, OR, Desert Research Institute: Reno, NV, June 1989.
(51) Middlebrook, A. M.; Murphy, D. M.; Thomson, D. S. *J. Geophys. Res.* **1998**, *103*, 16475−16483.
(52) Silva, P. J.; Prather, K. A. *Environ. Sci. Technol.* **1997**, *31*, 3074−3080.
(53) Silva, P. J.; Liu, D.-Y.; Noble, C. A.; Prather, K. A. *Environ. Sci. Technol.* **1999**, *33*, 3068−3076.

Received for review September 5, 2001. Revised manuscript received February 11, 2002. Accepted February 11, 2002.

ES0112700